Contents lists available at ScienceDirect

Chemical Engineering Research and Design

journal homepage: www.elsevier.com/locate/cherd

Heat integration for bio-oil hydroprocessing coupled with aqueous phase steam reforming

Mobolaji B. Shemfe, Beatriz Fidalgo, Sai Gu*,[1]*

Bioenergy & Resource Management Centre, Cranfield University, Bedford MK43 0AL, Bedfordshire, UK

ARTICLE INFO

Article history:
Received 19 June 2015
Received in revised form 6 August 2015
Accepted 8 September 2015
Available online 16 September 2015

Keywords:
Biorefinery
Heat integration
Fast pyrolysis
Steam reforming
Pinch analysis

ABSTRACT

Optimized heat exchanger networks can improve process profitability and minimize emissions. The aim of this study is to assess the heat integration opportunities for a hypothetical bio-oil hydroprocessing plant integrated with a steam reforming process *via* pinch technology. The bio-oil hydroprocessing plant was developed with rate based chemical reactions using ASPEN Plus® process simulator. The base case is a 1600 kg/h bio-oil hydroprocessing plant, which is integrated with a steam reforming process of the bio-oil aqueous phase. The impact of the reformer steam to carbon ratio on energy targets was analysed, revealing that significant energy savings can be achieved at different process variations. Aspen Energy Analyzer™ was employed to design the heat exchanger network. Two heat exchanger network designs are considered. The optimum design reveals that the second hydrodeoxygenation reactor effluent can preheat the bio-oil feed with minimal capital cost implication and achieve similar energy targets compared with the alternative design. The economic and environmental implications of the two heat exchanger network designs on product value were also evaluated.

1. Introduction

The impact of CO_2 emissions attributed to fossil fuel burning on escalating global temperatures has been the contention of the climate debate for the last three decades. In 2010, over 96% of global energy supply in the transport sector came from fossil fuel sources and contributed about 23% of global CO_2 emissions (WEC, 2011). In a race to mitigate the impact of CO_2 emissions on climate change, stakeholders are striving to implement stringent emission regulations, and support policies to enable the development of sustainable alternatives to fossil fuels (IPCC, 2014). According to the International Energy Agency, biofuels are projected to play a significant role in the energy transition by providing 27% of global transport fuel supply, with the aim of avoiding 2.1 $GtCO_2e$ by 2050 (IEA, 2011). As part of this gradual transition, the European Union has set a mandate to supply 10% of energy required in its transport sector from renewable sources by 2020 (IEA, 2010; JEC Biofuels Programme, 2014). To this end, the commercial deployment of biofuel production requires substantial research in process development, plant demonstrations and efficiency improvements to reduce production costs (IEA, 2011).

Biomass is one of the most readily available renewable fuel sources on the planet and has the potential to reduce net CO_2 emissions into the atmosphere due to its carbon neutrality. Biomass can be converted into energy mainly *via* chemical, biochemical and thermochemical processes (Naik et al., 2010). Although chemical and biochemical conversion processes including fermentation and transesterification have been demonstrated at different scales for producing first generation biofuels, they exert market pressure on food crops and threaten biodiversity (Naik et al., 2010; FAO, 2013). On the other

* *Corresponding authors.* Tel.: +44 2075949039.
E-mail addresses: b.fidalgofernandez@cranfield.ac.uk (B. Fidalgo), sai.gu@surrey.ac.uk (S. Gu).
[1] Current address: Department of Chemical and Process Engineering, University of Surrey, Guildford GU2 7XH, UK.
http://dx.doi.org/10.1016/j.cherd.2015.09.004
0263-8762/

hand, thermochemical conversion processes including pyrolysis, hydrothermal liquefaction, gasification, and combustion can be used to produce fuels, chemicals and heat from non-food crops with reduced threat to biodiversity and market prices. Among these thermochemical processes, fast pyrolysis presents the best case for liquid transport fuel production. Fast pyrolysis involves the thermochemical degradation of biomass in the absence of oxygen at temperatures ranging from 450 to 650 °C and at hot vapour residence time of approximately 2 s to maximize bio-oil production. The resultant bio-oil product has been demonstrated as a fuel for heat generation in boiler systems and for power generation in some diesel engines; however, it is incompatible with modern internal combustion engines due to its undesirable properties such as high oxygen content, low heating value and high acidity (Xiu and Shahbazi, 2012; Czernik and Bridgwater, 2004; Solantausta et al., 1993). Thus, upgrading is an essential step for bio-oil conversion into a usable fuel.

Bio-oil can be upgraded into transport fuels by two variants of conventional refinery processes *viz.* hydroprocessing and catalytic cracking (Bridgwater, 2012; Xiu and Shahbazi, 2012). Hydroprocessing involves hydrodeoxygenation and hydrocracking processes. Hydrodeoxygenation involves the catalytic rejection of oxygen atoms from the bio-oil organic compounds under mild operating conditions, while hydrocracking is a more severe hydroprocessing process, which involves the simultaneous catalytic cracking and hydrogenation of heavy hydrocarbon molecules into lighter hydrocarbon molecules (Gary and Handwerk, 1984). Furimsky (2000) comprehensively reviewed the historical catalyst development for the hydroprocessing of bio-oil obtained from various origins. Conventional catalysts including sulfided CoMo and NiMo have been used extensively for the hydrodeoxygenation of bio-oil with marginal product yields in the past. In recent research efforts, unconventional catalysts including transitional and noble metal carbides, nitrides, and phosphides are gaining more ground due to improved product yields (Furimsky, 2000, 2013). Nevertheless, the major challenges of bio-oil hydroprocessing include the high capital cost associated with hydrogen requirements and high-pressure operation, and catalyst deactivation due to coking (Cottam and Bridgwater, 1994; Furimsky, 2013). A significant quantity of hydrogen is required for the hydrogenation reactions of the aromatic rings present in the bio-oil oxygenates components (Furimsky, 2013). Succeeding the hydrodeoxygenation step, is the hydrocracking process, which breaks down heavy hydrocarbon molecules in the hydrodexoygenated oil into shorter chains hydrocarbons in the gasoline and diesel boiling point range. An alternative to the hydrocracking process is catalytic cracking, which is analogous to the fluid catalytic cracking of heavy gas oils in tradition refinery operations. It typically involves the heterolytic scission of the C—C covalent bonds to produced lighter hydrocarbon molecules at atmospheric pressure (Bridgwater, 2012). While catalytic cracking does not require hydrogen as in the case of hydrocracking, it is plagued by high rate of coke formation on active catalyst sites (Bridgwater, 2012). In order to reduce the additional operating cost of hydrogen required for bio-oil hydroprocessing and reduce excessive CO_2 emissions from sole hydrocarbon steam reforming, a steam reforming step of the bio-oil aqueous phase can be integrated with the process to generate hydrogen (Wang et al., 1997; Marker, 2005). Steam reforming of the hydrophilic organic components of bio-oil or the whole bio-oil product can be used to produce syngas, which is a mixture of hydrogen and carbon monoxide (van Rossum et al., 2007; Bimbela et al., 2009). Syngas can be utilized to supply hydrogen for hydroprocessing or, alternatively, it can be synthesized into liquid hydrocarbons through the Fischer–Tropsch process. The production of hydrogen and alkanes *via* the combined steam reforming and dehydration/hydrogenation of the bio-oil aqueous phase has also been demonstrated elsewhere (Huber and Dumesic, 2006).

Several techno-economic analyses of transport fuel production from bio-oil hydroprocessing integrated with steam reforming of bio-oil aqueous phase are available in literature (Cottam and Bridgwater, 1994; Wright et al., 2010; Brown et al., 2013; Shemfe et al., 2015). In a previous work of this group, the techno-economic analysis of a 72 MT/day fast pyrolysis plant and subsequent bio-oil hydroprocessing in a 1600 kg/h plant integrated with a steam reforming step of the aqueous phase was conducted (Shemfe et al., 2015). Operating cost was observed as an important economic input parameter that influenced product value to a significant extent. Product value was defined as the fuel product price at a net present value of zero over a 20 years period at 10% rate of return. It was observed that 10% and 20% increase/decrease in operating cost corresponded with 7% and 15% increase/decrease in product value, respectively. A significant percentage of this operating cost is attributed to utility cost. In this study, a methodical synthesis of the heat exchanger network (HEN) using Linnhoff's pinch technology is proposed with the aim of evaluating the effect of recovering heat from the process streams and the implications of HEN designs on the capital cost and operating cost of utilities. Two exchanger network (HEN) designs were developed and compare in terms of energy targets for a minimum driving temperature of 20 °C. The effect of steam to carbon ratio of the stream entering the main reformer on utility requirements, hydrogen product yield and cost performance was also investigated. Steam to carbon ratio is an important operating variable that dictates not only conversion in the reformer but also the amount of heat required for the process and the consequential steam savings.

2. Material and methods

2.1. Process description

The overall process is grouped into two main technical sections namely the bio-oil hydroprocessing and steam reforming sections as illustrated in Fig. 1. In the hydroprocessing section, the bio-oil feed undergoes hydrodeoxygenation (HDO) and hydrocracking operations. The hydrodeoxygenation reactions occur in two stages over Pt_2/Al_2O_3 catalyst (HDO-1 and HDO2). The product is subsequently fed into a flash drum (SP-1) to separate HDO gas phase from the HDO liquid phase. The resultant hydrodeoxygenated bio-oil is then fed into a phase separator (SP-1), where it is separated into two phases: an aqueous phase and a non-polar phase. The aqueous phase is fed to the reforming section to produce the hydrogen required for hydroprocessing, while the non-polar phase goes into the hydrocracking unit (HC-1) to produce compounds within the gasoline and diesel boiling point range. The product from the hydrocracker is finally fed into a product fractionator (HC-1) to separate its components into different product fractions. The reforming section comprises of a pre-reformer (SR-1) and a main steam reformer (SR-2) based on a process scheme proposed elsewhere (Marker, 2005). The bio-oil aqueous phase is

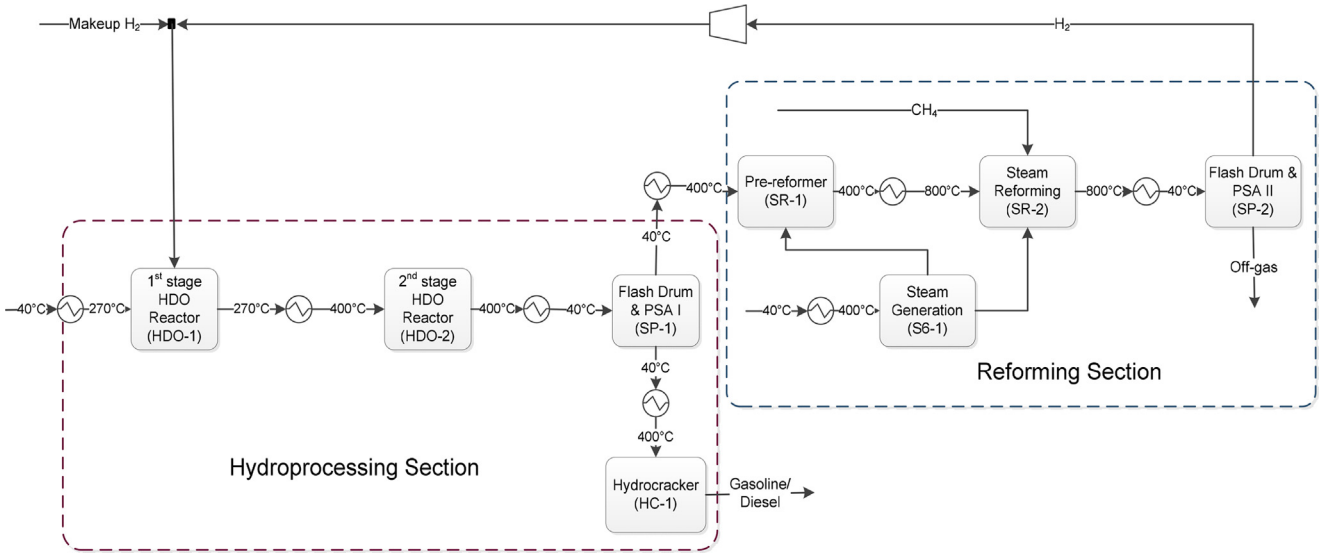

Fig. 1 – Simplified flow diagram of bio-oil hydroprocessing integrated with aqueous reforming.

fed into SR-1 along with superheated steam (from S6-1) to obtain a syngas mixture, which is subsequently fed to SR-2 along with additional steam and methane. The syngas produced in the main reformer is sent into a flash drum (SP-2), where the gas is separated from water, before being sent to a pressure swing adsorption unit (SP-2) to isolate hydrogen from the remaining gas mixture. The near purity hydrogen gas is compressed and recirculated to the hydroprocessing section.

2.2. *Model development*

A 1600 kg/h of bio-oil feed hydroprocessing plant model integrated with a steam reforming step of the bio-oil aqueous phase was developed in Aspen Plus® based on previous work of this group (Shemfe et al., 2015), and validated against experimental data reported in literature (Sheu et al., 1988). The inputs and assumptions adopted in model development are presented in Tables 1 and 2. Brief description of the model development is given below. Detailed model development can be found elsewhere (Shemfe et al., 2015).

2.2.1. *Model of the hydroprocessing section*

Briefly, bio-oil flow rate and composition were established from a 72 MT/day pinewood fast pyrolysis plant model. The two-stage hydrodeoxygenation process was modelled using two CSTRs based on kinetic parameters of a pseudo-first order reaction of lumped bio-oil components over Pt/Al_2O_3 catalyst (Sheu et al., 1988). For modelling purposes, the bio-oil feed was lumped into five pseudo-components based on their molecular weights and functional groups (light non-volatile; heavy non-volatile; phenolics; aromatics + alkanes); and coke + H_2O + outlet gas) in a yield reactor. The lumped bio-oil is introduced into the first stage hydrodeoxygenation reactor (HDO-1), which operates at 270 °C and 85 bar. The product stream from HDO-1 is subsequently fed into the second stage hydrodeoxygenation reactor (HDO-2), which operates at 380 °C and 87 bar in a hydrogen-rich environment of 5 wt. % of the total bio-oil feed (Marker, 2005; Wright et al., 2010). The product stream is then cooled down to 40 °C before entering the flash drum. Subsequently, the separated HDO liquid is fed to a phase separator, where the oil phase is separated from the aqueous phase. The oil phase is heated up to 400 °C and fed in the hydrocracker (HC-1), which operates at 104.3 bar to produce gasoline and diesel range fuels. The hydrocracker product composition was specified in a yield reactor based on experimental results reported by Elliott et al. (2009). The products from the hydrocracker go into a product fractionator, in which gasoline and diesel range products are separated.

Table 1 – Model inputs and assumptions.

Model parameter	Value
Bio-oil flow rate (kg/h)	1600
Steam to carbon ratio, main reformer	3:1
wt.% of bio-oil aqueous phase for reforming	40
H_2 PSA purity (%mol)	99
Exit temperature (°C), main reformer	800

Table 2 – Composition of bio-oil feedstock (Shemfe et al., 2015).

Component	(wt.%)	Functional group
Levoglucosan	48.39	Sugar
Water	20.61	Hydroxyl
Lignin Derivatives	12.47	Phenolic hydroxyl
Formaldehyde	3.43	Aldehyde
Hydroxyacetaldehyde	3.30	Aldehyde + hydroxyl
Methanol	2.69	Alcohol
Hydroxymethylfurfural	1.82	Aldehyde + alcohol
pCoumaryl	1.48	Phenol alcohol
Lumped phenolics	1.37	Phenolic hydroxyl
Ethanol	1.24	Alcohol
Acetone	1.08	Ketone
Phenol	0.74	Phenol
Glyoxal	0.64	Aldehyde
Xylan	0.36	Sugar
Acetaldehyde	0.14	Aldehyde
Acrylic	0.01	Carboxylic acid

2.2.2. *Model of the reforming section*

The aqueous phase from SP-1 goes to the steam reforming section in order to produce the hydrogen required for hydroprocessing. The pre-reformer feed is assumed to be 40 wt.% of the aqueous phase, which is fed along with superheated steam – supplied at 400 °C – in a 1:1 ratio to the

Table 3 – Hot and cold streams extracted from Simulation flowsheet.

Stream	Temperature (°C)		Specific heat (kJ/kg °C)	Heat capacity rate (kJ/°C h)	Heat Load (kW)
	Inlet	Outlet			
Hot streams					
HDO-2 effluent to SP-1	400	40	2.14	3623	362
SR-2 syngas to SP-2	800	45	2.80	4436	1214
Cold streams					
Bio-oil feed to HDO-1	25	270	2.40 (Goteti, 2010)	3859	263
HDO-1 effluent to HDO-2	270	400	2.40 (Goteti, 2010)	4062	147
Oil phase (SP-1) to HC-1	40	390	2.40	1426	139
Water feed to S6-1	25	400	4.20	5237	611
Aqueous phase (SP-1) to SR-1	40	400	2.40 (Goteti, 2010)	785	78
Steam to S6-1	400	800	2.20	2031	262
SR-1 effluent to SR-2	400	800	2.36	1225	169
Methane feed to SR-2	25	800	2.22	756	163

pre-reformer (SR-1) operating at 400 °C and 20 bar. SR-1 model was implemented using a Gibbs reactor, which calculates the product syngas composition at chemical equilibrium by minimizing Gibbs free energy. The exiting syngas was specified to comprise of H_2, CO, CO_2, CH_4 and H_2O, based on the underlying assumption that steam reforming (SR), water–gas shift and methanation reactions of bio-oil components occur in the pre-former as described by the following equations:

$$\text{Incomplete SR of aqueous phase} : C_nH_mO_k + (n-k)H_2O \leftrightarrow nCO + (n+m/2-k)H_2 \quad (1)$$

$$\text{Complete SR of aqueous phase} : C_nH_mO_k + (2n-k)H_2O \rightarrow nCO_2 + (2n+m/2-k)H_2O \quad (2)$$

$$\text{Water–gas shift reaction} : CO + H_2O \leftrightarrow CO_2 + H_2 \quad (3)$$

$$\text{Methanation reaction} : CO + 3H_2 \leftrightarrow CH_4 + H_2O \quad (4)$$

The exiting pre-reformer gas, a supplementary methane feed of 300 kg/h, and superheated steam are fed to the main steam reformer (SR-2) in a steam to carbon (S/C) ratio of 3:1. Steam and methane supplied to SR-2 were heated to 800 °C in order to avoid non-isothermal mixing of the streams and to mitigate untapped heat recovery opportunities. SR-2 model was also implemented by a Gibbs reactor, with the products specified as H_2, CO, CO_2, CH_4 and H_2O. The syngas produced in SR-2 is quenched to 40 °C and then fed to the flash drum, where the gas mixture is separated from the water vapour. The gas from the flash drum is then sent to the pressure swing adsorption unit, which separates hydrogen from off-gas at 99% purity. The hydrogen gas is compressed and sent to the hydroprocessing section for bio-oil upgrading.

Aspen Energy Analyzer® was used to design the heat exchanger network (HEN) schemes and to determine their implications on heating and cooling targets, and total cost performance accordingly. HEN designs were developed based on heat flow rate inequality and stream splitting rules achieved through tick-off heuristics. The total cost was estimated from both the energy cost of utilities and the capital cost of the heat exchangers. The capital cost of the heat exchangers was determined by the number of units and the minimum network area requirement (Linnhoff and Flower, 1982; Linnhoff and Hindmarsh, 1983). A comprehensive methodology for heat integration of biorefinery processes is well-documented by Sadhukhan et al. (2014).

Table 3 summarizes the thermodynamic data obtained from the Aspen Plus process simulation that were used to formulate the heat integration problem. The mean specific heat capacity of bio-oil from pine wood was assumed to be 2.40 kJ/kg K (Goteti, 2010). The approximation of the specific heat capacity of the bio-oil streams, which can vary considerably depending on process conditions specified in the upstream fast pyrolysis process, is a limitation of the present study. The specific heat capacities of the syngas streams exiting the pre-reformer and the steam reformer were estimated based on the pure gas composition weighted with their mole fractions as described by Poling et al. (2001).

2.3. *Economic analysis*

Economic analysis was conducted in Aspen Process Economic Analyser® V8.2 (APEA) based on Q1. 2013 cost data. APEA sizes process equipment and estimates capital and operating expenditures from material costs and wage rates. Key economic inputs and assumptions from a previous study of this group were adopted in the present work (Shemfe et al., 2015). The capital and operating cost extracted from APEA was used to determine the product value of the gasoline and diesel products. Product value is defined as product price at net present value of zero over plant life of 20 years at 10% rate of return. The hypothetical plant location is Northwest England. Consequently, material costs and wage rates in the UK were adopted as provided in APEA's UK cost template. The bio-oil transportation cost was not considered as it was assumed that the upstream fast pyrolysis plant is situated at the same location with the hydroprocessing plant. The capital cost of the heat exchanger network was estimated by the cost law described in Eq. (5), which is based on the minimum heat exchanger surface area requirement and number of shells using the default cost parameters provided in Aspen Energy Analyser®. The total utility cost was estimated from the following equation:

$$\text{HENCapitalCost} = a + b(\text{HeatExchangerArea}/\text{NoofShells})^{c \times \text{noofshells}} \quad (5)$$

$$\text{TotalUtilityCost} = \sum \text{Duty} \times \text{unitcost} \quad (6)$$

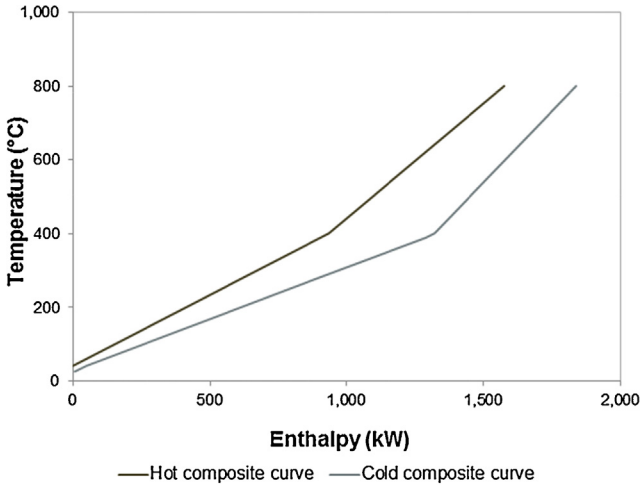

Fig. 2 – Composite curves (ΔT_{min} = 20 °C).

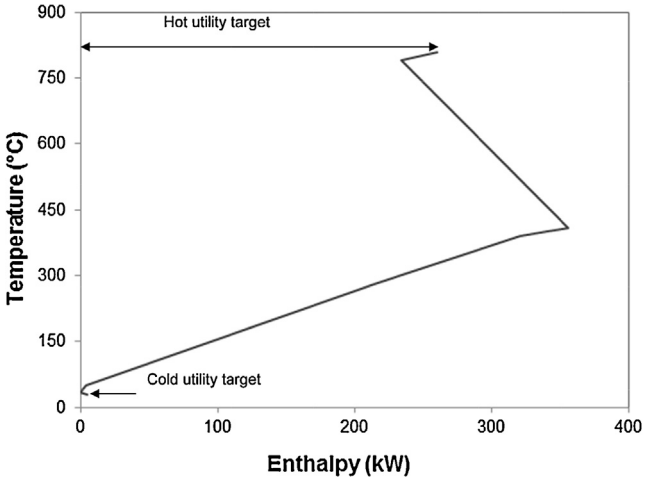

Fig. 3 – Grand composite curve (ΔT_{min} = 20 °C).

where *a*, *b*, and *c* are 10,000, 800 and 0.8, respectively. Furthermore, net CO_2 emission attributed to hot utility was estimated from European Commission Decision 2007/589/EC (European Commission, 2007) with natural gas specified as fuel source for the fired heaters.

3. Results and discussion

3. Results and discussion

3.1. *Heat integration*

The thermodynamic data extracted from the simulation provided in Table 3 were used to develop the composite curves (CC) and grand composite curve (GCC) for minimum driving temperatures (ΔT_{min}) of 0, 5, 10, 15 and 20 °C. The composite curves and grand composite curve for a ΔT_{min} = 20 °C are depicted as a case in point in Figs. 2 and 3, respectively.

From the CC and GCC of the different ΔT_{min}, the minimum energy requirements for hot and cold utilities were determined. Fig. 4 shows the relationship between the energy requirements and the minimum driving temperature. Fig. 4 exhibits a threshold problem *i.e.* utility requirement remains constant below the threshold driving temperature ($\Delta T_{threshold}$). $\Delta T_{threshold}$ is depicted by the dotted line at 15 °C. Generally for threshold problems; the optimum ΔT_{min} can only occur at or above $\Delta T_{threshold}$. A minimum driving temperature of 20 °C was selected for subsequent analysis. At this ΔT_{min}, the energy target for the hot utility is 260 kW, and that for cold utility is 5 kW. The minimum heat exchanger area and minimum heat exchanger units were estimated to be 290 m^2 and 11 units, respectively, from the CC. Higher ΔT_{min} were discarded because the further decrease in area requirement would imply a significant increase in utility and total cost.

3.2. *Steam to carbon ratio*

Table 4 summarizes the effect of the steam to carbon (S/C) ratio of the stream entering the main reformer on various key process parameters for a minimum driving temperature of 20 °C. S/C ratios of 3, 4 and 5 were evaluated. S/C ratio lower than 3 were not evaluated as they would promote coke formation in the reformer (Md Zin et al., 2015). As expected hot utility target increased with increasing S/C ratio, as more heat duty is required to generate additional steam to the reformer.

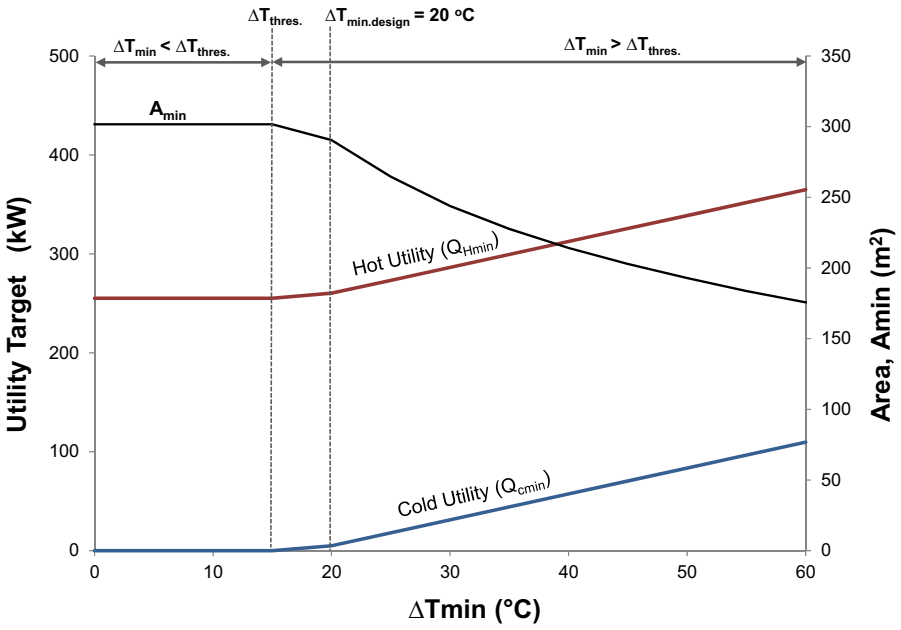

Fig. 4 – Hot and cold utility targets at different ΔT_{min}.

Table 4 – Effect of S/C on utility requirements, hydrogen yield and cost target.

Parameter	Case 1	Case 2	Case 3
S/C ratio	3	4	5
Hot utility target (kW)	260	313	389
Cold utility target (kW)	5	5	5
H_2 yield (kt/yr)	0.74	0.82	0.95
Utility cost (£/yr)	23,034	27,680	31,784

Consequently, utility cost also increased. Conversely, S/C had no impact on cold utility target. Hydrogen production increased with increasing S/C as the supply of more steam into the reformer favours an increase in the conversion of CH_4 into syngas. A S/C ratio of 3 was selected for subsequent analysis due to the significant increment of the hot utility target and cost with S/C ratio.

3.3. *Heat exchanger network design and performance*

Two heat exchanger networks were designed and their performances in terms of energy target for a driving temperature of 20 °C were compared: (i) HEN design 1 – utilization of second hydrotreater effluent to pre-heat the bio-oil feed to the hydrotreaters; and, (ii) HEN design 2 – utilization of second hydrotreater effluent to pre-heat steam feed to the pre-reformer. Figs. 5 and 6 show the grid diagrams of the hot and cold streams and heat recovery matches for HEN designs 1 and 2, respectively. The grid diagram was divided at the pinch temperature, which is 45 °C for above the pinch and 25 °C below the pinch. Design, economic and environmental performance indicators for HEN designs 1 and 2 are shown in Table 5.

As can be seen in Table 5, HEN design 1, which involved the utilization of the waste heat available in the second hydrodexogenation reactor effluent to preheat the bio-oil feed to the

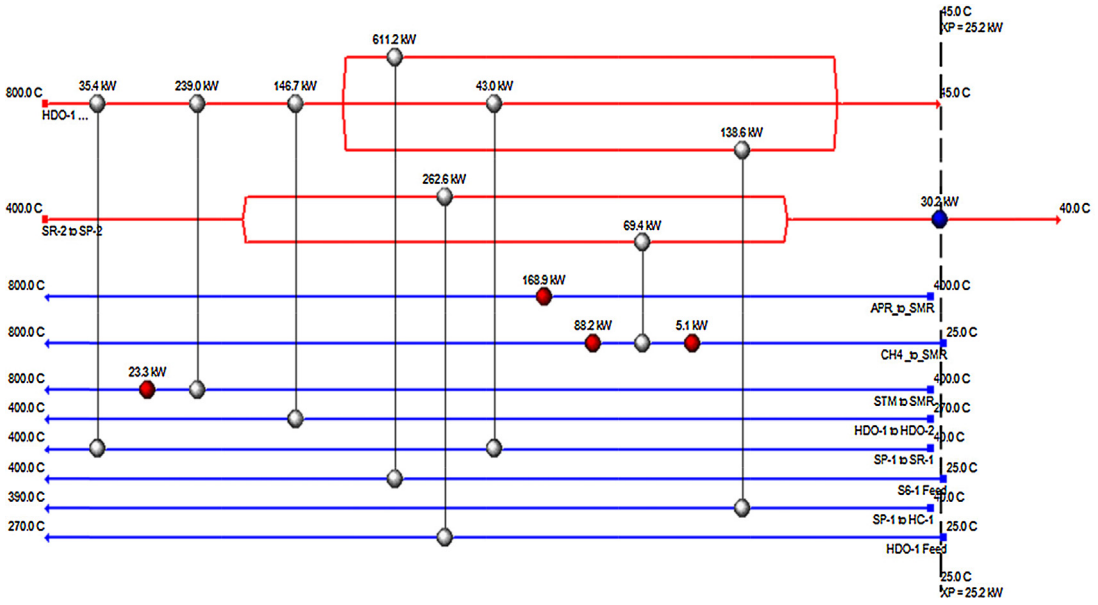

Fig. 5 – Grid diagram for HEN design 1: utilization of second hydrotreater (HDO-2) effluent to pre-heat the bio-oil feed to the 1st hydrotreater (HDO-1).

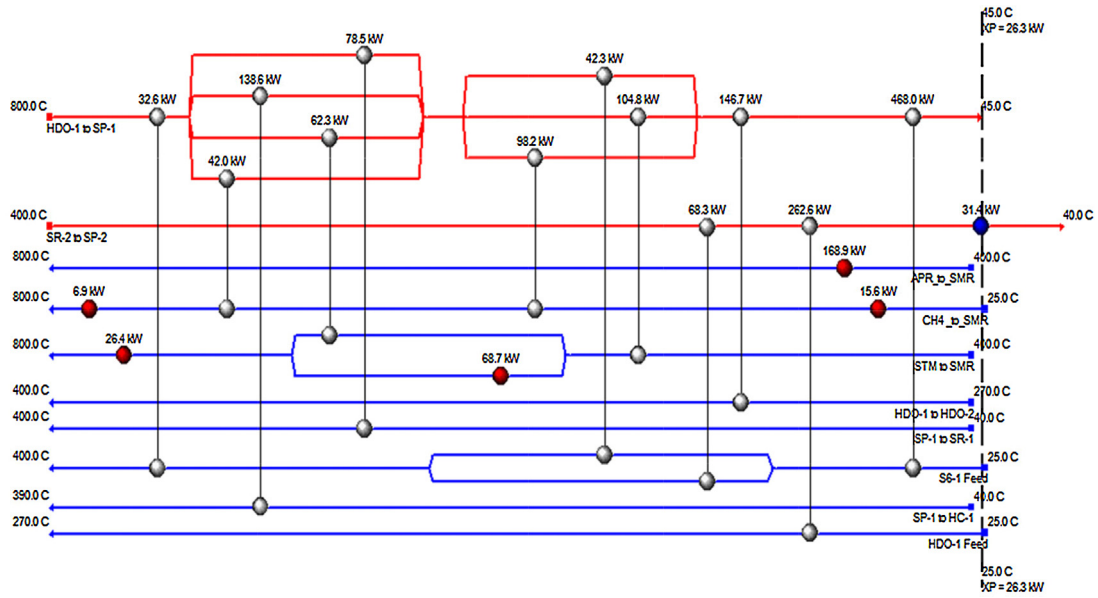

Fig. 6 – Grid diagram of HEN design 2: utilization of second hydrotreater (HDO-2) effluent to preheat the steam feed to the pre-reformer (SR-1).

Table 5 – Performance indicators of HEN designs 1 and 2.

HEN performance indicators	Non-integrated design	Design 1	Design 2
Hot utility fraction of target	–	1.01	1.10
Cold utility fraction of target	–	6.00	6.24
HEN area (m^2)	–	325	596
Capital cost of HEN (£)	–	200,310	314,622
Utility operating cost (£/yr)	235,401	25,374	25,481
Reduction in utility cost (%)	–	89	89
Utility % of total OPEX (%)	6.0	0.7	0.7
Total cost (£/yr)	–	95,153	133,213
Reduction in product value (%)	–	1.9	1.4
CO_2 emission (kt/yr)	4.5	0.50	0.51

first hydrodeoxygenation reactor, showed better economic performance than HEN design 2. Although 0.4% reduction in hot utility requirement was observed in HEN design 1 compared with HEN design 2, main differences were due to the difference in capital cost. Design 1 resulted in significantly less overall network area requirement and consequently a lesser capital cost than HEN design 2.

The annual operating cost of the non-integrated plant was estimated at £3.9 million, which accrues from the raw material costs, operating labour cost, maintenance cost, supervision cost, and utility cost. The utility cost is 6% of the annual operating cost, which is estimated at £235,401 per year It is worth noting that the utility cost with the incorporation of HEN designs 1 and 2 was £25,374 per year and £25,481 per year, respectively. Therefore, the hypothetical implementation of a heat exchanger network could reduce 89% of the annual utility cost compare to a non-integrated scheme.

Discounted cash flow analysis revealed a product value of £6.38 per gasoline gallon equivalent (GGE) at a net present value (PV) of zero over a plant life of 20 years for the non-integrated design. The economic implication of decreased utility cost due to the incorporation of HEN designs 1 and 2 resulted in 1.9% and 1.4% reduction in PV, respectively. Moreover, the CO_2 emission attributed to hot utility were estimated at 4.5 kt/yr for the non-integrated design and 0.5 kt/yr for integrated HEN design. Consequently, the implementation of HEN could reduce 89% of the annual CO_2 emissions.

4. Conclusions

This study assessed various energy saving opportunities for a hypothetical 1600 kg/h bio-oil hydroprocessing plant integrated with steam reforming model developed in Aspen Plus®.

Thermodynamic data extracted from Aspen Plus simulation was used to formulate the heat integration problem. Pinch technology was used to determine the minimum utility demands. Composite and grand composite curves revealed hot and cold utility targets of 260 kW and 5 kW, respectively, for a minimum driving temperature of 20 °C and steam to carbon (S/C) ration of 3 in the main reformer. This ΔT_{min} was selected as the optimum minimum driving temperature for heat exchanger network design because of an existing threshold problem.

Better energy and cost performance were observed with a S/C ratio of 3 compared to other values investigated (S/C = 4 and 5).

HEN synthesis according to stream matching constraints revealed that the utilization of waste heat from the second hydrodeoxygenation reactor effluent to preheat bio-oil feed to the first hydrodeoxygenation reactor (HEN design 1) gives better economic performance than its utilization to preheat the steam feed to the pre-reformer (HEN design 2). Both HEN designs exhibited similar performance in meeting heating and cooling requirements; however, HEN design 1 resulted in less capital cost. Moreover, HEN design 1 enhanced profitability of the process by achieving around 2% reduction in product value and almost 90% in CO_2 emission attributed to the hot utility.

Acknowledgements

The authors gratefully acknowledge the financial support for this work by the UK Engineering and Physical Sciences Research Council (EPSRC) project reference: EP/K036548/1 and FP7 Marie Curie iComFluid project reference: 312261.

References

Bimbela, F., Oliva, M., Ruiz, J., García, L., Arauzo, J., 2009. Catalytic steam reforming of model compounds of biomass pyrolysis liquids in fixed bed: acetol and *n*-butanol. J. Anal. Appl. Pyrolysis 85 (1–2), 204–213.

Bridgwater, A.V., 2012. Review of fast pyrolysis of biomass and product upgrading. Biomass Bioenergy 38 (0), 68–94.

Brown, T.R., Thilakaratne, R., Brown, R.C., Hu, G., 2013. Techno-economic analysis of biomass to transportation fuels and electricity via fast pyrolysis and hydroprocessing. Fuel 106 (0), 463–469.

Cottam, M.L., Bridgwater, A.V., 1994. Techno-economic modelling of biomass flash pyrolysis and upgrading systems. Biomass Bioenergy 7 (1–6), 267–273.

Czernik, S., Bridgwater, A.V., 2004. Overview of applications of biomass fast pyrolysis oil. Energy Fuels 18 (2), 590–598.

Elliott, D.C., Hart, T.R., Neuenschwander, G.G., Rotness, L.J., Zacher, A.H., 2009. Catalytic hydroprocessing of biomass fast pyrolysis bio-oil to produce hydrocarbon products. Environ. Prog. Sustainable Energy 28 (3), 441–449.

European Commission, 2007. European Commission decision 2007/589/EC. Off. J. Eur. Comm. 50, L229/1.

FAO, Food and Agriculture Organization of the UN, 2013. FAO Food Price Index, Available at ⟨http://www.fao.org/worldfoodsituation/foodpricesindex/en/⟩ (accessed 03/27).

Furimsky, E., 2000. Catalytic hydrodeoxygenation. Appl. Catal., A: Gen. 199 (2), 147–190.

Furimsky, E., 2013. Hydroprocessing challenges in biofuels production. Catal. Today 217 (0), 13–56.

Gary, J., Handwerk, G., 1984. Petroleum Refining Technology and Economics, second ed. Marcel Dekker Inc, New York, NY.

Goteti, A., 2010. Experimental Investigations and Systems Modeling of Fractional Catalytic. Pyrolysis of Pine. Georgia Institute of Technology, Atlanta.

Huber, G.W., Dumesic, J.A., 2006. An overview of aqueous-phase catalytic processes for production of hydrogen and alkanes in a biorefinery. Catal. Today 111 (1–2), 119–132.

IEA, 2010. Sustainable Production of Second-Generation Biofuels: Potential and Perspectives in Major Economies and Developing Countries. IEA, Paris, France.

IEA, 2011. Technology roadmap: biofuels for transport. In: Tech Rep., International Energy Agency. International Energy Agency, Paris.

IPCC, 2014. Summary for policymakers. In: Climate Change 2014, Mitigation of Climate Change. Contribution of Working Group III to the Fifth Assessment Report of the Intergovernmental Panel on Climate Change. Cambridge University Press, Cambridge, United Kingdom and New York, NY, USA.

JEC Biofuels Programme, 2014. EU renewable energy targets in 2020: revised analysis of scenarios for transport fuels. In: EUR 26581 EN. European Commission, Luxembourg.

Linnhoff, B., Flower, J.R., 1982. User Guide on Process Integration for the Efficient Use of Energy. The Institution of Chemical Engineers, Rugby.

Linnhoff, B., Hindmarsh, E., 1983. The pinch design method for heat exchanger networks. Chem. Eng. Sci. 38 (5), 745–763.

Marker, T.L., 2005. Opportunities for biorenewables in oil refineries. In: Final Technical Report. The United States. DOEGO15085. UOP, Des Plaines, IL.

Md Zin, R., Ross, A.B., Jones, J.M., Dupont, V., 2015. Hydrogen from ethanol reforming with aqueous fraction of pine pyrolysis oil with and without chemical looping. Bioresour. Technol. 176, 257–266.

Naik, S.N., Goud, V.V., Rout, P.K., Dalai, A.K., 2010. Production of first and second generation biofuels: a comprehensive review. Renewable Sustainable Energy Rev. 14 (2), 578–597.

Poling, B.E., Prausnitz, J.M., O'Connell, J.P., 2001. The Properties of Gases and Liquids, fifth ed. New York, NY, McGraw-Hill.

Sadhukhan, J., Ng, K.S., Martinez-Hernandez, E., 2014. Heat integration and utility system design. In: Biorefineries and Chemical Processes: Design, Integration and Sustainability Analysis, first ed. Wiley, Chichester, pp. 63–91.

Shemfe, M.B., Gu, S., Ranganathan, P., 2015. Techno-economic performance analysis of biofuel production and miniature electric power generation from biomass fast pyrolysis and bio-oil upgrading. Fuel 143 (0), 361–372.

Sheu, Y.E., Anthony, R.G., Soltes, E.J., 1988. Kinetic studies of upgrading pine pyrolytic oil by hydrotreatment. Fuel Process. Technol. 19 (1), 31–50.

Solantausta, Y., Nylund, N., Westerholm, M., Koljonen, T., Oasmaa, A., 1993. Wood-pyrolysis oil as fuel in a diesel-power plant. Bioresour. Technol. 46 (1–2), 177–188.

van Rossum, G., Kersten, S.R.A., van Swaaij, Wim P.M., 2007. Catalytic and noncatalytic gasification of pyrolysis oil. Ind. Eng. Chem. Res. 46 (12), 3959–3967.

Wang, D., Czernik, S., Montane, D., Mann, M., Chornet, E., 1997. Biomass to hydrogen via fast pyrolysis and catalytic steam reforming of the pyrolysis oil or its fractions. Ind. Eng. Chem. Res. 36 (5), 1507–1518.

WEC, 2011. Global Transport Scenarios 2050. World Energy Council, London, United Kingdom, ISBN 978-0-946121-14-4.

Wright, M.M., Daugaard, D.E., Satrio, J.A., Brown, R.C., 2010. Techno-economic analysis of biomass fast pyrolysis to transportation fuels. Fuel 89 (Suppl. 1), S2–S10.

Xiu, S., Shahbazi, A., 2012. Bio-oil production and upgrading research: a review. Renewable Sustainable Energy Rev. 16 (7), 4406–4414.